Accepted Manuscript

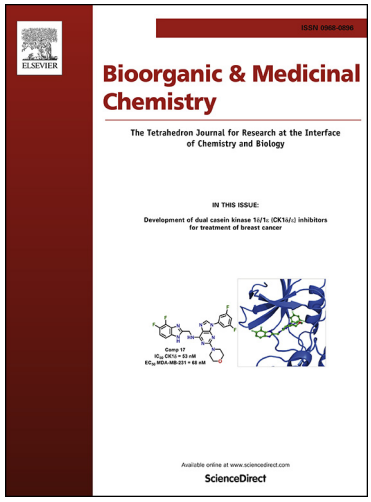

Discovery of isatin and 1H-indazol-3-ol derivatives as D-amino acid oxidase (DAAO) inhibitors

Bence Szilágyi, Péter Kovács, György G. Ferenczy, Anita Rácz, Krisztina Németh, Júlia Visy, Pál Szabó, Janez Ilas, György T. Balogh, Katalin Monostory, István Vincze, Tamás Tábi, Éva Szökő, György M. Keserű

PII: S0968-0896(17)32415-X
DOI: https://doi.org/10.1016/j.bmc.2018.02.004
Reference: BMC 14190

To appear in: *Bioorganic & Medicinal Chemistry*

Received Date: 12 December 2017
Revised Date: 27 January 2018
Accepted Date: 3 February 2018

Please cite this article as: Szilágyi, B., Kovács, P., Ferenczy, G.G., Rácz, A., Németh, K., Visy, J., Szabó, P., Ilas, J., Balogh, G.T., Monostory, K., Vincze, I., Tábi, T., Szökő, E., Keserű, G.M., Discovery of isatin and 1H-indazol-3-ol derivatives as D-amino acid oxidase (DAAO) inhibitors, *Bioorganic & Medicinal Chemistry* (2018), doi: https://doi.org/10.1016/j.bmc.2018.02.004

Graphical Abstract

To create your abstract, type over the instructions in the template box below.
Fonts or abstract dimensions should not be changed or altered.

Discovery of Isatin and 1H-indazol-3-ol Derivatives as D-Amino Acid Oxidase (DAAO) Inhibitors

Leave this area blank for abstract info.

Bence Szilágyi, Péter Kovács, György G. Ferenczy, Anita Rácz, Krisztina Németh, Júlia Visy, Pál Szabó, Janez Ilas, György T. Balogh, Katalin Monostory, István Vincze, Tamás Tábi, Éva Szökő, György M. Keserű*
Research Centre for Natural Sciences, Hungarian Academy of Sciences, Magyar tudósok krt. 2. H-1117 Budapest, Hungary

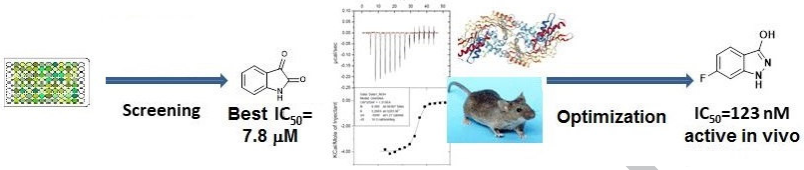

ELSEVIER

Bioorganic & Medicinal Chemistry
journal homepage: www.elsevier.com

Discovery of isatin and 1H-indazol-3-ol derivatives as D-amino acid oxidase (DAAO) inhibitors

Bence Szilágyi[a], Péter Kovács[a], György G. Ferenczy[a], Anita Rácz[a], Krisztina Németh[b], Júlia Visy[a], Pál Szabó[c], Janez Ilas[d], György T. Balogh[e], Katalin Monostory[f], István Vincze[g], Tamás Tábi[g], Éva Szökő[g], György M. Keserű[a]*

[a]*Medicinal Chemistry Research Group, Research Centre for Natural Sciences, Hungarian Academy of Sciences, Magyar tudósok krt. 2. H-1117 Budapest, Hungary;*
[b]*Chemical Biology Research Group, Research Centre for Natural Sciences, Hungarian Academy of Sciences, Magyar tudósok krt. 2. H-1117 Budapest, Hungary*
[c]*MS Metabolomics Laboratory, Core Facility, Research Centre for Natural Sciences, Hungarian Academy of Sciences, Magyar tudósok krt. 2. H-1117 Budapest, Hungary*
[d]*University of Ljubljana, Faculty of Pharmacy, Aškerčeva 7, 1000 Ljubljana, Slovenia*
[e]*Compound Profiling Laboratory, Gedeon Richter plc. Gyömrői út 30-32, H-1103 Budapest, Hungary*
[f]*Metabolic Drug-Interactions Research Group, Institute of Enzymology, Research Centre for Natural Sciences, Hungarian Academy of Sciences, Magyar tudósok krt. 2. H-1117 Budapest, Hungary*
[g]*Department of Pharmacodynamics, Semmelweis University, Nagyvárad tér 4. Budapest, H-1089, Hungary*

ARTICLE INFO

Article history:
Received
Received in revised form
Accepted
Available online

Keywords:
D-amino acid oxidase
Optimization
Protonation state
Binding thermodynamics

ABSTRACT

D-amino acid oxidase (DAAO) is a potential target in the treatment of schizophrenia as its inhibition increases brain D-serine level and thus contributes to NMDA receptor activation. Inhibitors of DAAO were sought testing [6+5] type heterocycles and identified isatin derivatives as micromolar DAAO inhibitors. A pharmacophore and structure-activity relationship analysis of isatins and reported DAAO inhibitors led us to investigate 1H-indazol-3-ol derivatives and nanomolar inhibitors were identified. The series was further characterized by pK_a and isothermal titration calorimetry measurements. Representative compounds exhibited beneficial properties in in vitro metabolic stability and PAMPA assays. 6-fluoro-1H-indazol-3-ol (**37**) significantly increased plasma D-serine level in an in vivo study on mice. These results show that the 1H-indazol-3-ol series represents a novel class of DAAO inhibitors with the potential to develop drug candidates.

* Corresponding author. Tel.: +36-1-382-6821; e-mail: gy.keseru@ttk.mta.hu

1. Introduction

D-amino acid oxidase (DAAO) is a flavoprotein that catalyses the oxidative deamination of D-amino acids. Genetic studies have found association between schizophrenia and single nucleotide polymorphisms in the DAAO and its regulator (G72)[1]. Furthermore, DAAO expression and enzyme activity have been reported to be increased in post mortem brain tissue samples from patients with schizophrenia compared to healthy controls[2]. Moreover reduced D-serine levels were described in the serum and cerebrospinal fluid of schizophrenic patients, therefore it has been suggested that the inhibition of DAAO could ameliorate schizophrenic symptoms, especially with the co-administration with D-serine[3,4]. D-serine, a D-amino acid that is regulated by DAAO, is a potent, endogenous co-agonist of the N-methyl-D-aspartic acid (NMDA) receptor[5]. Because NMDA receptor dysfunction is thought to be involved in the positive (psychotic), negative and cognitive symptoms in schizophrenia, there has been much interest in developing potent and selective DAAO inhibitors for the treatment of this disease. Until now several DAAO inhibitors were reported, including 5-methylpirazole-3-carboxylic acid **1**[6,7], 4H-furo[3,2-b]pyrrole-5-carboxylic acid **2**[8], 4H-thieno[3,2b]pyrrole-5-carboxylic acid **3**[9], 3-hydroxyquinolin-2(1H)-one **4**[10], 1-hydroxy-1H-benzo[d]imidazol-2(3H)ones **5**[11], and 6-chlorobenzo[d]isoxazol-3-ol (CBIO) **6**[4] (Figure 1).

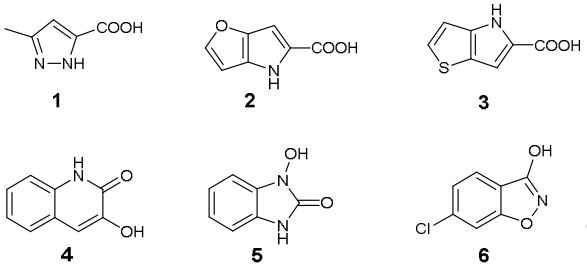

Figure 1. Chemical structure of DAAO inhibitors.

Compounds **1**-**3** are examples of inhibitors that contain a carboxylic acid moiety similarly to endogenous ligands. Significant effort has been devoted to identify inhibitors that do not contain carboxylic acid (see e.g. compounds **4**-**6**) and having beneficial pharmacokinetic profile. However, the DAAO binding site prefers small and highly polar ligands and this seriously limits ligand variability. Moreover, although the binding pocket features an Arg residue as a key interaction site the incorporation of non-carboxylic acid Arg binder motifs[12] into DAAO inhibitors did not prove to be a straightforward strategy. Thus, it still remains a significant challenge to find inhibitors with reasonable affinity and balanced pharmacokinetic properties.

In this paper we report novel sets of DAAO inhibitors having isatin and 1H-indazol-3-ol scaffolds. The latter chemotype was optimized to nanomolar inhibitors that were further evaluated in ADME tests and an in vivo proof of concept assay.

2. Results and discussion

Our initial analysis of known DAAO inhibitors revealed that most of the chemotypes are small and polar mono- or bicyclic compounds having an acidic functionality (Figure 1). Consequently, in the first round of searching for new inhibitor scaffolds we screened [6+5] type heterocycles of this type. .All compounds contain the pharmacophore elements of the reference compounds in different arrangements. **Table *1*** shows the inhibitory activity of tested compounds together with two reference inhibitors, namely CBIO (**6**)[4], and BIO (**7**)[4] Most of the scaffolds showed no activity at 20 µM concentration against DAAO except for compounds **9**, **11** and **16**. Since **9** and **16** showed only moderate activity we selected the isatin scaffold (**11**) for further evaluation (Table 2).

Table 1 [6+5] type heterocyclic compounds tested for DAAO inhibition.

Compound	Structure	Inhibition % at 20µM[a]	Compound	Structure	Inhibition % at 20µM[a]
6 (CBIO)	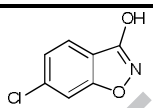	114 (3)	**7 (BIO)**	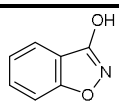	101 (2)
8[13]	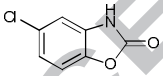	-38 (2)	**9**[13]	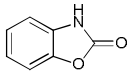	26 (1)
10[14]	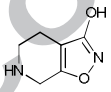	-42 (1)	**11**[15]	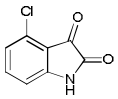	46 (6)
12[16]	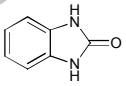	-5 (2)	**13**[17]	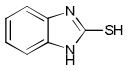	1 (0)
14[18]	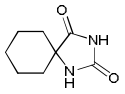	-1 (1)	**15**[19]	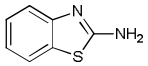	-27 (0)
16[20]	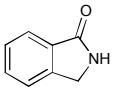	26 (1)	**17**[19]	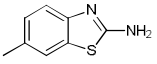	-4 (4)

[a] All measurements were performed n=2; standard deviation in percentage is shown in parenthesis

Table 2. DAAO inhibitory activity of isatin analogues.

Compound	Structure	IC_{50} [μM] **or** % inhibition at 20μM[a]	Compound	Structure	IC_{50} [μM] **or** % inhibition at 20μM[a]
18[15]	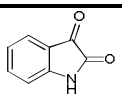	19% (1)	**22**[21]	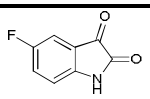	49% (7)
11[15]	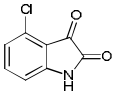	46% (6)	**23**[22]	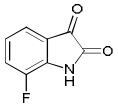	12% (2)
19[15]	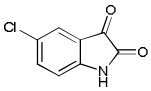	13% (2)	**24**[23]	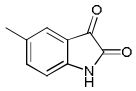	8% (3)
20[15]	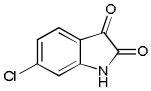	-1% (1)	**25**[23]	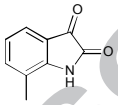	13.1 (20)
21[15]	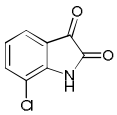	7.87 (7)			

[a] All measurements were performed n=2; standard deviation in percentage is shown in parenthesis

Haloscan resulted in **21** as the most active derivative that is behind the reference compounds. Although we got similar potency for **25** the 7-fluoro derivative (**23**) was found to be much active. The SAR inconsistency together with the order of magnitude higher IC_{50} values compared to reference compounds made further optimization of this scaffold less promising. In order to improve the potency of compound **21** we decided to modify the pharmacophore elements of the isatin scaffold (Figure 2).

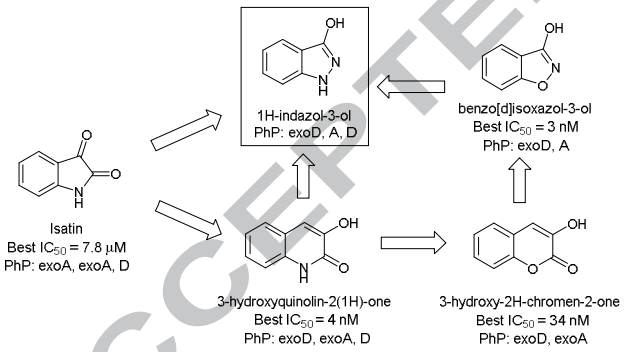

Figure 2. Design paradigm leading to the 1H-indazol-3-ol scaffold. Abbreviations: PhP, pharmacophore; exoA – H-bond acceptor in exo position; A, acceptor; exoD H-bond donor in exo position; D, donor.

Comparative analysis of the available DAAO-inhibitor co-crystal structures revealed that all of the known inhibitors bind to Arg283 forming H-bonding interactions with the guanidine NHs. Considering the positively charged character of the Arg headgroup these interactions could be improved significantly forming a negatively charged moiety on the scaffold. This has been realized in the case of the 3-hydroxyquinolin-2(1H)-one scaffold that contains a deprotonable enol instead of the upper carbonyl group of the isatin scaffold. It is interesting to note that the corresponding 3-hydroxy-2H-chromen-2-one scaffold was found to be somewhat less active against DAAO indicating that the donor adjacent to the aromatic ring might be beneficial. Comparing the binding modes of these compounds revealed the formation of an extra H-bond between the NH of the 3-hydroxyquinolin-2(1H)-one and the backbone carbonyl of Gly313 (Figure 3).

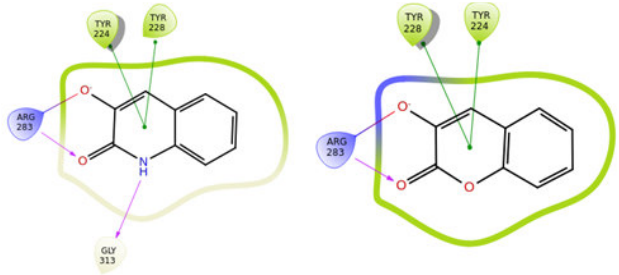

Figure 3. Experimental binding modes of 3-hydroxyquinolin-2(1H)-one and 3-hydroxy-2H-chromen-2-one scaffolds.

Contracting the six membered ring of these compounds we obtain two [6+5] type scaffolds as the benzo[d]isoxazol-3-ol (see e.g. **7**) and the 1H-indazol-3-ol (see e.g. **28**). Although the former one turned to be very potent DAAO inhibitors, the latter has not been investigated yet. Consequently, our chemistry program aimed at the exploration of the 1H-indazol-3-ol scaffold. To achieve this goal, we prepared several 1H-indazol-3-ol fragments (Table 3).

Table 3. DAAO inhibitory activity of 1H-indazol-3-ol fragments.

Compound	Structure	IC_{50} [μM] **or** % inhibition at 20μM[a]	Compound	Structure	IC_{50} [μM] **or** % inhibition at 20μM[a]
26[24]	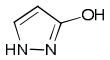	0% (0)	**27**	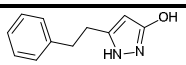	66% (2)
28	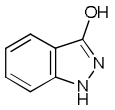	not measurable[b]	**29**	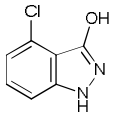	19% (8)
30	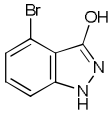	34% (0)	**31**	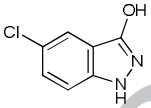	not measurable[b]
32	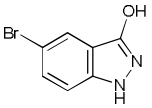	not measurable[b]	**33**	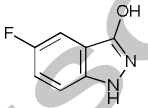	not measurable[b]
34	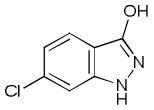	0.15 (13)	**35**	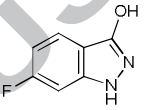	0.12 (42)
36	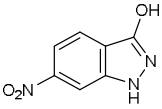	1.20 (25)	**37**	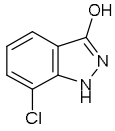	10.1 (13)

[a] All measurements were performed n=2; standard deviation in percentage is shown in parenthesis
[b] Strong autofluorescence

Although the 1H-pyrazol-3-ol (**26**) showed no activity both the phenetyl (**27**) and the condensed 1H-indazol-3-ol derivatives were found to be inhibitors of the target. 1H-indazol-3-ols substituted in position 6 or 7 had significant activity, of which 6-chloro (**34**) and 6-fluoro-1H-indazol-3-ol (**35**) exhibited near to low nanomolar inhibition. An analysis of reported potent DAAO inhibitors suggests that they are all able to deprotonate under slightly basic conditions (pH~8) where DAAO works optimally. In order to better characterize the 1H-indazol-3-ol series we determined the pK_a value for several representative compounds (Table 4).

Table 4. Measured pKa values of representative compounds

Cmpd	pK_a	SD	% of deprotonated microspecies[a] (pH=7.4)	% of deprotonated microspecies[a] (pH=8)
21	9.44	0.106	3.96	14.1
28	8.16	0.004	21.5	52.2
29	7.51	0.004	38.7	71.6
30	7.51	0.002	35.7	68.8
31	7.53	0.006	25.0	57.0
34	7.59	0.009	21.7	52.5
35	7.84	0.001	19.3	48.8
36	6.52	0.005	32.8	64.7
37	7.28	0.007	22.0	52.9

[a] calculated by the ChemAxon pKa plugin

The pK_a values of the investigated compounds are typically between 7 and 8 suggesting that they are at least partially deprotonated at slightly basic pH. This appears to be a common property of DAAO inhibitors and also of the endogenous ligand. Whether the compounds bind to the enzyme in a deprotonated form depends on the local environment within the binding pocket, however, our free energy perturbation calculations (data not shown) strongly suggest that the bound compounds of the 1H-indazol-3-ol series are deprotonated and are carrying a negative charge. This finding, in fact, explains the reduced affinity of isatins (the measured pK_a value of **21** is 9.44 and it has a low fraction of ionized microspecies at pH 7.4). We also note, that the substituents of the benzole ring of the 1H-indazol-3-ol series affect pK_a on one hand, and influences affinity via its interactions with DAAO, on the other hand.

Table 5. Dissociation constants (K_d) from ITC and inhibitory activity (IC_{50}) from D-kynurenine assay.

Cmpd	IC_{50} [μM][a]	K_d porcine ITC [μM]
4		0.15 (0.03)
CBIO(6)	0.027 (36)	0.87 (0.03)
BIO (7)	0.418 (9.0)	0.44 (0.14)
25	13.140 (13)	8.23 (1.46)
28	-	4.43 (1.63)
31	-	0.78 (0.24)
32	-	3.29 (0.81)

33	-	1.20 (0.50)
34	0.156 (13)	2.00 (0.40)
35	0.123 (42)	1.00 (0.10)
36	1.205 (25)	4.59 (1.73)
37	10.139 (13)	3.31 (0.54)

[a]All measurements were performed n=2; standard deviation in percentage is shown in parenthesis

Some compounds, although potentially active based on structural similarity to those having significant DAAO inhibitory potency could not be measured owing to strong autofluorescense. Here it is worth noting that the D-kynurenine test[25] was selected for activity measurements because of the assay interference[26] observed for the 1H-indazol-3-ol compounds with the HRP[27] test commonly applied to measure DAAO inhibitory activity. Compounds that could not be measured in the D-kynurenine test either owing to autofluorescence were subjected to isothermal titration calorimetric (ITC) affinity determination (Table 5). Moreover, compounds that exhibited significant inhibitory activity in the D-kynurenine test were also measured with ITC so that relation between in vitro activity and ITC affinity scales could be established.

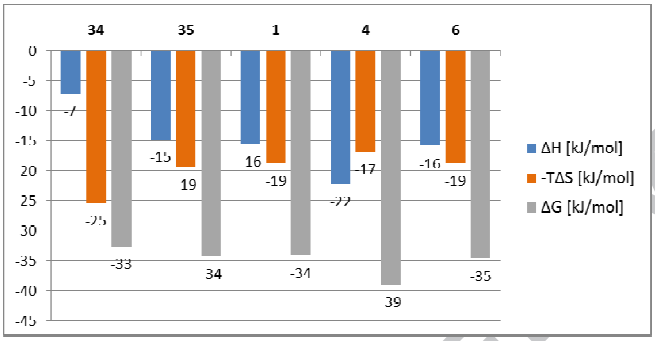

Figure 4 Binding thermodynamic profiles of 1H-indazol-3-ols (**34**, **35**) and reference DAAO inhibitors (**1**, **4** and **6**).

Dissociation constants (K_d) and inhibitory activities in Table 5 change parallel and compounds **31** and **33** that were not measurable in the D-kynurenine test show K_d values similar to compounds exhibiting inhibitory activity lower than 1 µM IC_{50}. This finding shows that 5-substitution is advantageous and results in inhibitory potency comparable to those of 6-substituted compounds.

It is remarkable that although 3-hydroxyquinolin-2(1H)-one with an extra H-bond donor with respect to 3-hydroxy-2H-chromen-2-one is more active (*cf.* Figure 2) benzo[d]isoxazol-3-ol derivatives appear to be less active than 1H-indazol-3-ol derivatives although the former compounds have an extra H-donor in a similar position (*cf.* e.g. compounds **28** and **6**). An explanation for this observation is proposed by the comparison of the complex structure of docked **28** with the X-ray structure of 3-hydroxyquinolin-2(1H)-one (PDB: 3G3E). The arginine binding moieties (NCO- in **28** and OCCO- in 3G3E) are slightly shifted resulting in larger separation between Arg283 and N in **28** versus Arg283 and O in 3G3E. Moreover, there is also a slight shift in the position of the ring NH-groups resulting in a suboptimal H-bond between **28** and Gly313 backbone carbonyl.

The analysis of the thermodynamic profiles (Figure 4) showed that the binding of **34** is more entropically driven as compared to **35** and also to CBIO (**6**). In fact, the thermodynamic profiles of **35** and **6** are very similar. Interestingly, the compound equipped with the six membered ring (**4**) was found to be the only enthalpy driven DAAO inhibitor in this set of compounds. The high entropy content of binding supports that these compounds bind in deprotonated form, since the desolvation of charged species upon binding has increased advantageous entropic contribution to the binding free energy.[28] Contracting the six membered ring as in compounds **34** and **35** resulted in some decrease in affinity and also significant improvements in entropic contribution of **34**.

The advantageous in vitro potency of several 1H-indazol-3-ol compounds prompted us to further investigate their properties relevant for advanced leads. Compounds **34** and **35** with IC_{50}=156 nM and 123 nM, respectively were selected for PAMPA test to characterize absorption properties and microsomal/hepatocyte stability to characterize metabolic stability. According to the PAMPA test the 6-Cl derivative (**34**) shows high and the 6-F derivative (**35**) shows medium permeability. These data demonstrate that these compounds, and more generally, appropriately substituted derivatives in the 1H-indazol-3-ol series have potentially advantageous intestinal absorption. Metabolic stability of compounds **34** and **35** in mouse and human hepatic microsomes as well as in mouse and human hepatocytes was also investigated.

Table 6 Effective permeability (Pe*10^{-6}cm/s) of representative compounds of the 1H-indazol-3-ol series

Compound	grad-pH 5.5-7.4				grad-pH 6.5-7.4				iso-pH 7.4				Permeability
	P_e	SD	MR%	SD	P_e	SD	MR%	SD	P_e	SD	MR%	SD	category
34	9.53	0.34	6.7	0.5	7.43	0.90	9.7	0.3	4.47	0.29	2.5	1.1	High
35	1.20	0.01	3.9	1.3	0.97	0.12	7.1	1.5	0.72	0.13	5.8	1.5	Medium

Data in Table 7

Table 7 show that these compounds are stable against first pass metabolism and predict highly favourable bioavailability.

Table 7 Microsomal and hepatocyte stability and predicted bioavailability of representative compounds of the 1H-indazol-3-ol series

	34	**35**

	Mouse microsomes	Mouse hepatocytes	Human microsomes	Human hepatocytes	Mouse microsomes	Mouse hepatocytes	Human microsomes	Human hepatocytes
t1/2[a] (min)	56.51	52.21	215.90	450.38	79.52	178.32	182.34	411.51
Cl_{int}[b] (mL/min/kg)	11.67	68.19	0.76	2.54	8.29	19.96	0.90	2.78
Cl_H[c] (mL/min/kg)	9.504	29.275	0.714	2.075	7.137	14.371	0.835	2.232
F[d] (%)	93.981	81.459	97.966	94.087	95.480	90.898	97.619	93.637

[a] elimination half-life; [b] intrinsic clearance; [c] hepatic clearance; [d]bioavailability

Based on the beneficial in vitro DAAO inhibitory activity, good predicted absorption and metabolic stability we selected compound **35** for measuring its in vivo effect on mice D-serine level (Figure 5). It was found that the co-administration of **35** and D-serine results in a significant ($p<0.05$) increase of the D-serine level compared to the administration of D-serine alone (33% increase after 10 minutes and 27% increase after 60 minutes with corresponding blood levels of 13.1 µM and 0.77 µM of **35**, respectively).

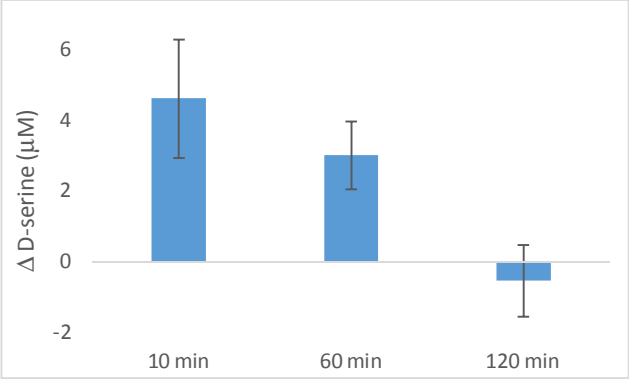

Figure 5 Difference in mice D-serine level in the presence and absence of compound **35**.

3. Conclusion

Inhibitors of D-amino acid oxidase were sought using a fragment based approach. Based on the structure of reported DAAO inhibitors [6+5] type heterocyclic compounds were selected for measuring their DAAO inhibitory potency. This led to the identification of the isatin scaffold based compounds as weak DAAO inhibitors. Structure-activity studies of isatins including a haloscan resulted in compounds at most around 8 µM activity. Therefore, we decided to change the scaffold using pharmacophore and structure-activity analysis of DAAO inhibitors and we arrived at the 1H-indazol-3-ol scaffold not yet tested against DAAO. Several 1H-indazol-3-ol derivatives were prepared and nanomolar inhibitors were identified. pK_a measurements of several representatives show that although these compounds are less acidic than the majority of known DAAO inhibitors they are at least partially deprotonated at pH=8 that corresponds to the optimal activity of DAAO. Compounds whose activity could not be measured with the applied enzymatic assay due to strong autofluorescense were subjected to isothermal titration calorimetry (ITC) measurements to determine their affinity towards DAAO. ITC measurements identified compounds with comparable affinity to the best inhibitors found by the enzymatic assay. Two representative compounds 6-chloro-1H-indazol-3-ol (**34**) and 6-fluoro-1H-indazol-3-ol (**35**) exhibited good permeability in PAMPA assay and good stability in mouse and human microsomes as well as in mouse and human hepatocytes. In an *in vivo* study, 6-fluoro-1H-indazol-3-ol (**35**) significantly increased plasma D-serine level in mice. These results show that the 1H-indazol-3-ol series represents a novel class of DAAO inhibitors with the potential to serve as a basis for developing drug candidates.

4. Experimental

4.1. Chemistry

4.1.1. General information

Melting points were determined on an Optimelt SRS (Standard Research Systems) and are uncorrected. NMR measurements were performed on Varian NMR System 500 spectrometer, 1H and 13C NMR spectra were measured at room temperature (30 °C) in an appropriate solvent. 1H and 13C chemical shifts are expressed in parts per million (δ) referenced to TMS or residual solvent signals. Compounds **6**, **7**, **10** were purchased from Sigma-Aldrich, compounds **11**, **18**, **19**, **20**, **21**, **22**, **23**, **24**, **25** were purchased from Combi-Blocks. Reactions were monitored with Merck silica gel 60 F254 TLC plates (0.25 mm thickness). All the chemicals and solvents were used as supplied. High resolution mass spectrometric measurements were performed using a Q-TOF Premier mass spectrometer (Waters Corporation, Milford, MA, USA) in positive electrospray ionization mode.

*4.1.2. 5-phenethyl-1H-pyrazol-3-ol (**27**)*

560 mL (11.5 mmol) hydrazine monohydrate was added dropwise to a stirred solution of 2.5 g (11.3 mmol) ethyl 3-oxo-5-phenylpentanoate in 25 mL of ethanol. Stirring was continued for 90 min more. Solvent was removed and diethyl ether (20 mL) was added, then the syrup was crystallized and filtrated. 1,33 g (6.89 mmol, 61%) white powder was obtained, mp: 167-169°C. ^{1}H NMR (500 MHz, DMSO-d6) δ 2.70 – 2.79 (m, 2H), 2.82 – 2.89 (m, 2H), 5.24 (s, 1H), 7.14 – 7.23 (m, 3H), 7.27 (t, J = 7.4 Hz, 2H), 10.37 (brs, 2H). ^{13}C NMR (125 MHz, DMSO-d6) 27.5, 34.5, 88.2, 125.9, 128.3, 141.1, 143.7, 160.8; HRMS (ESI): $(M+H)^+$ calcd for $C_{11}H_{13}N_2O^+$, 189.1028; found, 189.1028

4.1.3. General procedure for synthesis of 1H-indazol-3-ols

The solution of sodium nitrite was added dropwise to a continuously stirred and ice cooled suspension of anthranilic acid in water and conc. hydrochloric acid, at such a rate that the temperature remains below 5°C. After the sodium nitrite was all been added, stirring was continued for 30 min more and a solution of sodium sulfite in water was added all at once. After 2h conc. hydrochloric acid was added and the mixture was stirred

overnight. Then it was slowly heated to 80°C and kept at this temperature for 2h. After cooling to room temperature, the pH was adjusted to 5.5 with 1M sodium hydroxide. The precipitate was filtered and triturated with small amount of ethanol.

*4.1.4. 4-chloro-1H-indazol-3-ol (**29**)*

1.89 g (11.0 mmol) 2-amino-6-chlorobenzoic acid in 10 mL water – 2.2 mL conc. hydrochloric acid; 760 mg (11.0 mmol) $NaNO_2$ in 1.7 mL water; 3.75 g Na_2SO_3 (29.7 mmol) in 16.5 mL water; 3.3 mL conc. hydrochloric acid; 447 mg (24%) solid product, mp: 188-191°C. ^{1}H NMR (500 MHz, DMSO-d6) δ 6.95 (dd, *J* = 5.3, 2.7 Hz, 1H), 7.21 – 7.25 (m, 2H), 11.78 (s, 1H) ; ^{13}C NMR (125 MHz, DMSO-d6) 109.2, 109.3, 118.9, 125.6, 127.8, 143.2, 154.6; HRMS (ESI): $(M+H)^+$ calcd for $C_7H_6N_2OCl^+$, 169.0169; found, 169.0167

*4.1.5. 7-chloro-1H-indazol-3-ol (**37**)*

1.5 g (8.7 mmol) 2-amino-3-chlorobenzoic acid in 8 mL water – 1.8 mL conc. hydrochloric acid; 603 mg (8.7 mmol) $NaNO_2$ in 1.4 mL water; 2.97 g Na_2SO_3 (23.5 mmol) in 13.1 mL water; 2.6 mL conc. hydrochloric acid; 36 mg (2.4%) solid product, mp: 150-153°C. ^{1}H NMR (500 MHz, DMSO-d6) δ 6.98 (t, *J* = 7.7 Hz, 1H), 7.39 (d, *J* = 7.4 Hz, 1H), 7.60 (d, *J* = 8.0 Hz, 1H), 10.87 (s, 1H), 11.96 (s, 1H) ; ^{13}C NMR (125 MHz, DMSO-d6) 114.3, 114.7, 119.0, 119.5, 126.2, 139.0, 155.9; HRMS (ESI): $(M+H)^+$ calcd for $C_7H_6N_2OCl^+$, 169.0169; found, 169.0169

4.2. Enzyme inhibition assay

D-2-Amino-4-(2-aminophenyl)-4-oxobutanoic acid (D-kynurenine) was used to measure D-amino acid oxidase activity according to the protocol described in ref. 25. The measurements were carried out on a Citation3 cell imaging multi-mode microplate reader (BioTek Instruments, Inc., Winooski, VT, USA) with 364 well plates. The applied wavelengths were 340 nm and 396 nm. The buffer contained 20 mM TRIS-HCl and 100 mM NaCl. Human DAAO was purchased from TargetEx Ltd. (Dunakeszi, Hungary) and kept in 1 µg/10 µL aliquots at -80 °C.

4.3. Molecular modeling

Crystal structures of hDAAO were retrieved from the Protein Data Bank and were processed with Schrödinger's protein preparation wizard[29]. Ligands were prepared with Ligprep[29] and docked by Glide[29]. Best scored complexes were visually inspected to select compounds for in vitro enzyme inhibition assay.

4.4. Isothermal titration calorimetry (ITC)

ITC measurements were carried out against porcine DAAO (purchased from Calzyme Laboratories, Inc., San Luis Obispo, CA, USA) on a MicroCal ITC200 microcalorimeter (Malvern Instruments, Worcestershire, UK). The buffer contained 100 mM TRIS-HCl, 150 mM NaCl, 0.25 mM TCEP, 50 µM FAD, 1% V/V DMSO and 0.02% V/V Tween 20. After being dissolved in the buffer at a concentration of 100 µM (verified on a NanoDrop 1000 spectrophotometer), the protein was kept in 300 µL aliquots at -20°C. Prior to the ITC measurements, the protein solution was thawed, the ligand was dissolved in the same buffer at a concentration of 1 mM, and both solutions were thoroughly degassed. The DAAO solution was loaded into the sample cell and was titrated at 25°C with the ligand solution. Injection volumes were between 0.8 and 2.8 µL during the measurements and a total of 13 points were acquired per curve (excluding the first injection of 0.4 µL). The stirring rate was set to 600 rpm and the time between injections was 200 s.

4.5. Metabolic stability test

4.5.1. Isolation of hepatocytes and microsomes

Mouse and human primary hepatocytes or hepatic microsomes were used in *in vitro* pharmacokinetic experiments. The hepatocytes or microsomes were pooled from 6 mice or from 3 human subjects. Male NMRI mice were purchased from Toxi-Coop Toxicological Research Center (Budapest, Hungary), whereas human liver tissues were obtained from organ-transplant donors at the Department of Transplantation and Surgery, Semmelweis University (Budapest, Hungary). The liver cells were isolated using collagenase perfusion method of Bayliss and Skett.30] Briefly: The liver tissues were perfused through the portal vein with Ca^{2+}-free medium (Earle's balanced salt solution) containing EGTA (0.5 mM) and then with the same medium without EGTA, finally with the perfusate containing collagenase (Type IV, 0.25 mg/mL) and Ca^{2+} at physiological concentration (2 mM). The perfusion was carried out at pH 7.4 and at 37°C. Softened liver tissue was gently minced and suspended in ice-cold hepatocyte dispersal buffer. Hepatocytes were filtered and isolated by low-speed centrifugation (50xg), and washed three times. The yield and percent of cell viability according to the trypan blue exclusion test were determined.[31] For pharmacokinetic studies, the hepatocytes were suspended at $2x10^6$ cells/mL concentration in culture medium[32]. Hepatic microsomal fractions were prepared from pooled hepatocytes. The cells were homogenized in 0.1 M Tris-HCl buffer (pH 7.4) containing 1 mM EDTA and 154 mM KCl. Microsomes were prepared by differential centrifugation as described by van der Hoeven and Coon.[33] All procedures of preparation were performed at 0-4°C. Microsomal protein content was determined by the method of Lowry et al.[34] with bovine serum albumin as the standard.

*4.5.2. In vitro pharmacokinetics of **34** and **35***

Time courses of the unchanged pharmacons (**34** and **35**) in hepatocytes and in hepatic microsomes were obtained. Each compound was incubated with cell suspension (2×10^6 cells/mL) or with microsomes (4 mg/mL) at 37°C in a humid atmosphere containing 5% CO_2. The parent compounds were added directly to the cell culture medium or to 0.1 M Tris-HCl buffer (pH 7.4) at the final concentration of 1 µM. The microsomal incubation mixtures contained an NADPH-regenerating system (1 mM NADPH, 10 mM glucose 6-phosphate, 5 mM $MgCl_2$ and 2 units/mL glucose 6-phosphate dehydrogenase). At various time points (at 0, 15, 30, 45, 60, 90, 120, 180, 240 min for hepatocyte incubations; at 0, 15, 30, 45, 60, 90 min for microsomal incubations), the incubation mixtures were sampled (aliquots: 0.25 mL) and terminated by the addition of 0.17 mL ice-cold acetonitrile containing the internal standard, carbamazepine (0.13 µM). The cell and microsomal debris was separated by centrifugation, and the supernatant was analysed by LC-MS/MS for quantitation of the parent compound.

4.5.3. Estimation of pharmacokinetic parameters

The intrinsic clearance (Cl_{int}) for hepatocytes [mL/(min×$2x10^6$cells)] and for microsomes [mL/(min×4mg)] was calculated from the decrease in the concentration of the parent compound as follows[35]:

$$Cl_{\text{int}} = \frac{D}{AUC}$$

where the dose (D) was the target 1 nmol (in 1 mL) and

$$AUC = \frac{B}{\beta}$$

The concentration at 0 min (B) was 1 μM (1 nmol/mL) and β was determined by fitting exponential using the measured drug-candidate disappearance. Since in our case D was numerically equal to B, and Cl_{int} was numerically equal to β

$$Cl_{int} = \beta = \frac{\ln 2}{t_{1/2}}$$

For scaling up the Cl_{int} value to obtain $Cl_{int\ per\ whole\ liver\ (g)/bw\ (kg)}$, the cell or microsomal protein concentration in the liver (cell number in mouse liver: $1.35x10^8$cells/g liver, in human liver: $1.39x10^8$cells/g liver; microsomal protein concentration in mouse liver: 50 mg/g liver, in human liver: 40 mg/g liver), the ratio of the average liver weight and average body weight parameters (for mouse: 76.1 g/kg; for human: 23.7 g/kg) were used. The value for predicted hepatic clearance (Cl_H) was calculated as follows[36,37]:

$$Cl_H = \frac{Cl_{\text{int}\,liver/bw} * fu * Q_{plasma}}{(Cl_{\text{int}\,liver/bw} * fu) + Q_{plasma}}$$

where the flow rate of $Q_{plasma}=Q_H*plasma/blood\ ratio$. To calculate Cl_H, the hepatic flow rate (for mouse: 90 mL/min/kg; for human: 20 mL/min/kg), plasma/blood ratio=0.57 and fu=1 values were used[38]. (Q_H is the hepatic blood flow, while *fu* is the unbound fraction of the compound.) The bioavailability (%) was determined by using the equation[39]:

$F=(1-E)*100.$

where E is the hepatic extraction ratio[36,40]:

$E=Cl_H*Q_H$

4.6. Parallel artificial membrane permeability assay (PAMPA) method

A slightly modified version of the parallel artificial membrane permeability assay[41] was used to determine the effective permeability (P_e, cm/s). A 96-well acceptor plate (Multiscreen Acceptor Plate, MSSACCEPTOR; Merck-Millipore) and a 96-well filter plate (PVDF, Multiscreen™-IP, MAIPNTR10, pore size 0.45μm; Merck-Millipore) were assembled into a sandwich. The hydrophobic filter material of the 96 well filter plate was coated with 5 μl of a 4 % (w/v) n-dodecane solution of phosphatidylcholine:cholesterol (2:1). Subsequently, the acceptor wells at the bottom of the sandwich were filled with 300 μL of 10 mM PBS solution adjusted to pH 7.4. The donor wells at the top of the sandwich were hydrated with 150 μL of test compound solution. The test compound solution was prepared by diluting x100 from a 10 mM stock solution in DMSO using PBS solution at pH 5.5, pH 6.5 or pH 7.4 followed by filtration through a MultiScreen Solubility filter plate. The resulting sandwich was then incubated at 37 °C for 4h. After the incubation, PAMPA sandwich plates were separated and compound concentrations in donor and acceptor solutions were determined by HPLC-DAD.

The effective permeability and membrane retention of molecules were calculated by the following equations[42]:

$$P_e = \frac{-2{,}303}{A \cdot (t - \tau_{SS})} \cdot \frac{(V_A \cdot V_D)}{(V_A + V_D)} \cdot \lg\left[1 - \left(\frac{V_A + V_D}{(1 - MR) \cdot V_D}\right) \cdot \left(\frac{C_D(t)}{C_D(0)}\right)\right]$$

where P_e is the effective permeability coefficient (cm/s), A is the filter area (0.3 cm^2), V_D and V_A are the volumes in the donor (0.15 mL) and acceptor phase (0.3 mL), t is the incubation time (s), τ_{SS} is the time (s) to reach steady-state, $C_D(t)$ is the concentration (M) of the compound in the donor phase at time t, $C_D(0)$ is the concentration (M) of the compound in the donor phase at time 0, MR is the membrane retention factor:

$$MR = \left(1 - \frac{C_D(t)}{C_D(0)} - \frac{V_A}{V_D}\frac{C_A(t)}{C_D(0)}\right)$$

In the case of gradient-pH conditions (donor: 5.5 → acceptor: 7.4 and donor: 6.5 → acceptor: 7.4) the effective permeability of compounds was calculated by the following gradient-pH equation:

$$P_e = \frac{-2{,}303}{A \cdot (t - \tau_{SS})} \cdot \left(\frac{1}{1 + r_a}\right) \cdot \lg\left[-r_a + \left(\frac{1 + r_a}{1 - MR}\right) \cdot \frac{C_D(t)}{C_D(0)}\right]$$

r_a is the sink asymmetry ratio (gradient-pH-induced), defined as

$$r_a = \left(\frac{V_D}{V_A}\right)\frac{P_e^{(A \to D)}}{P_e^{(D \to A)}}$$

.

Quantitative chromatographic analysis for PAMPA was performed on a SHIMADZU Prominence Modular HPLC system (Shimadzu Corporation, Japan), equipped with a vacuum degasser, a binary pump, a Nexera SIL-30ACMP Multiplate Autosampler, a column oven and controlled with LabSolutions software (Version 5.53 SP2). Chromatographic analysis was performed at 40 °C on a Kinetex 2.6 μm C18 100A (30 x 3.0 mm) column with a mobile phase flow rate of 1.1 mL/min. Composition of mobile phase A was 0.1% (v/v) formic acid in water, mobile phase B was the mixture of acetonitrile and water 95/5 (v/v) with 0.1% (v/v) formic acid. The following linear gradient program was applied: 0 min 0% B, 0.3 min 0% B, 1.8 min 100% B, 2.4 min 100% B, 2.41 min 0%. This was followed by a 1.2 min equilibration period prior to the next injection corresponding to approximately 3.6 min total analysis time per sample. Chromatograms were recorded at 220±4 nm and the applied injection volume was 4 μL.

4.7. pK_a measurement

All pK_a determinations were carried out in aqueous medium. The proton-dissociation constants were determined by UV-spectrophotometric titration method using D-PAS technique (Sirius Analytical Instruments Ltd., Forest Row, UK; attached to a Sirius T3 instrument.[43,44] The pK_a values were calculated by Refinement Pro™ software. Absorbancies in the spectral region of 250-450 nm were used in the analysis. All measurements were performed in solutions of 0.15M KCl under nitrogen atmosphere, at 25.0 ± 0.5 °C. All pK_a values were measured in 6 replicates.

4.8. In vivo pharmacology

4.8.1. Animal studies

Male NMRI mice of 25-30 g were purchased from Toxi-Coop Toxicological Research Center (Budapest, Hungary). The animals were housed in an air-conditioned (22 +/- 2 °C) animal room with 12 h light and dark cycle. They had free access to standard laboratory rodent chow and water. Five mice per group

were treated intraperitoneally with 30 mg/kg D-serine in the absence or presence of 30 mg/kg **35** dissolved in 5% DMSO containing saline. The test compound and D-serine were administered simultaneously. After 10, 20, 30, 60, 120, 240 and 360 minutes the mice were anesthetized by carbon dioxide, decapitated and their blood was collected using EDTA as anticoagulant. Plasma was obtained by centrifugation at 2000 g, 4 °C for 5 minutes and the samples were stored frozen at -80 °C until analysis.

4.8.2. Determination of D-serine plasma level

We used a chiral capillary electrophoresis laser induced fluorescence (CE-LIF) method developed in our laboratory for D-serine measurement[45]. Briefly, plasma was deproteinated by mixing with 3 volumes of ice cold acetonitrile followed by centrifugation at 3000 g, 4 °C for 20 min. The supernatant was spiked with 10^{-6} M L-cysteic acid as internal standard. 7-fluoro-4-nitro-2,1,3-benzoxadiazole (NBD-F, 2 mg/mL final concentration) was used for sample derivatization in pH 8.5 borate buffer at 65 °C for 20 min. Derivatized samples were diluted with 2 volumes of distilled water and injected to a Beckman P/ACE MDQ CE system controlled by 32 Karat software version 5.0 (Beckman Coulter, Brea, CA, USA) equipped with a LIF detector containing an Argon-ion laser source, with excitation and emission wavelengths of 488 and 520 nm, respectively. Separations were performed in fused silica capillary coated with linear polyacrylamide (75 µm id, 30/40 cm effective/total length) using 50 mM HEPES pH 6.5 separation buffer containing 6 mM 6-monodeoxy-6-mono(3-hydroxy)propylamino-β-CD (HPA-β-CD) as chiral selector. Injection was accomplished with pressure (3447 Pa for 5 s). The voltage applied was constant -28 kV. Temperature of the liquid capillary coolant was set at 15 °C. Before each run the capillary was rinsed with water and separation buffer.

Acknowledgments

This study was supported by the National Brain Research Program grant (project KTIA NAP_13). Celesztina Domonkos is acknowledged for help in biological measurements, Katalin Tóth and Máté Déri for performing *in vitro* pharmacokinetic studies and Judit Müller for the performing PAMPA tests.

Supplementary Material

^{1}H and ^{13}C NMR spectra of compounds **27-33** are available as supplementary information.

References and notes

1 Badner, J. A.; Gershon, E. S. *Mol. Psychiatry* **2002**, *7* (4), 405–411.
2 Burnet, P. W. J.; Eastwood, S. L.; Bristow, G. C.; Godlewska, B. R.; Sikka, P.; Walker, M.; Harrison, P. J. *Mol. Psychiatry* **2008**, *13* (7), 658–660.
3 Millan, M. J. *Psychopharmacology (Berl).* **2005**, *179* (1), 30–53.
4 Ferraris, D.; Duvall, B.; Ko, Y.-S.; Thomas, A. G.; Rojas, C.; Majer, P.; Hashimoto, K.; Tsukamoto, T.. *J. Med. Chem.* **2008**, *51* (12), 3357–3359.
5 Wolosker, H. *Mol. Neurobiol.* **2007**, *36* (2), 152–164.
6 Adage, T.; Trillat, A.-C.; Quattropani, A.; Perrin, D.; Cavarec, L.; Shaw, J.; Guerassimenko, O.; Giachetti, C.; Gréco, B.; Chumakov, I.; Halazy, S.; Roach, A.; Zaratin, P. *Eur. Neuropsychopharmacol.* **2008**, *18* (3), 200–214.
7 Lange, J. H. M.; Venhorst, J.; van Dongen, M. J. P.; Frankena, J.; Bassissi, F.; de Bruin, N. M. W. J.; Besten, C. den; de Beer, S. B. A.; Oostenbrink, C.; Markova, N.; Kruse, C. G. *Eur. J. Med. Chem.* **2011**, *46* (10), 4808–4819.
8 Sparey, T.; Abeywickrema, P.; Almond, S.; Brandon, N.; Byrne, N.; Campbell, A.; Hutson, P. H.; Jacobson, M.; Jones, B.; Munshi, S.; Pascarella, D.; Pike, A.; Prasad, G. S.; Sachs, N.; Sakatis, M.; Sardana, V.; Venkatraman, S.; Young, M. B. *Bioorg Med Chem Lett.* **2008**, 18, 3386–3391
9 Smith, S. M.; Uslaner, J. M.; Yao, L.; Mullins, C. M.; Surles, N. O.; Huszar, S. L.; McNaughton, C. H.; Pascarella, D. M.; Kandebo, M.; Hinchliffe, R. M.; Sparey, T.; Brandon, N. J.; Jones, B.; Venkatraman, S.; Young, M. B.; Sachs, N.; Jacobson, M. A.; Hutson, P. H. *J. Pharmacol. Exp. Ther.* **2009**, *328* (3) 921-930
10 Duplantier, A. J.; Becker, S. L.; Bohanon, M. J.; Borzilleri, K. A.; Chrunyk, B. A.; Downs, J. T.; Hu, L. Y.; El-Kattan, A.; James, L. C.; Liu, S.; Lu, J.; Maklad, N.; Mansour, M. N.; Mente, S.; Piotrowski, M. A.; Sakya, S. M.; Sheehan, S.; Steyn, S. J.; Strick, C. A.; Williams, V. A.; Zhang, L. *J. Med. Chem.* **2009**, *52* (11), 3576–3585.
11 Berry, J. F.; Ferraris, D. V; Duvall, B.; Hin, N.; Rais, R.; Alt, J.; Thomas, A. G.; Rojas, C.; Hashimoto, K.; Slusher, B. S.; Tsukamoto, T. *ACS Med. Chem. Lett.* **2012**, *3* (10), 839–843.
12 **Chan, A.W.E, Laskowski, R.A., Selwood, D.L.:** *J. Med. Chem.*, **2010**, 53 (8), pp 3086–3094
13 Bach A. , Pizzirani D. , Realini N. , Vozella V. , Russo D., Penna I., Melzig L., Scarpelli R. , and Piomelli D. : *J. Med. Chem.*, **2015**, 58 (23), pp 9258–9272
14 Patent application US4278676
15 Liu H.-Q., Wang D.-C., Wu F., Tang W. , Ouyang P.-K.: *Chinese Chemical Letters* **2013** 24 929–933
16 Staab, H.A. *Justus Liebigs Annalen der Chemie*, **1957**, 609, 75-82
17 Van Allan J. A.; Deacon B. D.: *Org. Synth. Coll.* Vol.4 **1963**, 569.
18 Herbst R.M.; Johnson T. B.: *J. Am. Chem. Soc*. **1932**, 54, 2463.
19 Telvekar V. N., Bachhav H. M., Bairwa V. K.: *SYNLETT* **2012**, 23, 2219–2222
20 Clift M. D., Silverman R. B *Bioorg. Med. Chem. Lett.,* **2008,** 18, 3122–3125
21 Yen V. Q., Buu-Hoi N. P., Xuong N. D. *J. Org. Chem.*, **1958**, 23, 1858–1861
22 Mckittrick B., Failli A., Steffan R. J., Soll R. M., Hughes P., Schmid J., Asselin A. A., Shaw C. C., Noureldin R. and Gavin G *J. Heterocyclic Chem.*, **1990,** 27, 2151
23 Boa A. N., Canavan S. P., Hirst P. R., Ramsey C., Stead A. M. W. and McConkey G. A. *Bioorg. Med. Chem.* **2005,** 13, 1945–1967
24 Huang H., Si P., Wang L., Xu Y., Xu X., Zhu J., Jiang H., Li W., L. Chen, and Li J *Chem. Med. Chem.* **2015** , 10 ,1184–1199
25 Song Z., Ogaya T., Ishii K., Ichiba H., Iizuka H., Fukushima T. *J. Health Sci. **2010,** 56, 341.*
26 1H-indazol-3-ols are oxidized in the presence of horseradish peroxidase and H2O2.
27 Cook S.P., Galve-Roperh I., Martinez del Pozo A., Rodriguez-Crespo I.:. *J. Biol. Chem*. **2002,** 277, 27782–27792.
28 Ferenczy, G. G.; Keserű, G. M. *Med. Chem. Commun.* **2016**, 7 (2), 332–337.
29 Schrödinger Suite 2016-1, Schrödinger, LLC, New York, NY, 2016.
30 Bayliss M.K., Skett P: Isolation and culture of human hepatocytes, in Human Cell Culture Protocolls (ed. Jones GE), Humana Press Totowa, New Jersey, USA **1996**. p 369-389.
31 Berry M.N., Edwards A.M., Barrit G.J.: Isolated hepatocytes, Elsevier Amsterdam, **1991**.
32 Ferrini J.B., Ourlin J.C., Pichard L., Fabre G., Maurel P.: Human hepatocyte culture, in Cytochrome P450 protocols (eds. Phillips IR and Shephard AE), Humana Press Totowa, New Jersey, USA **1998**. p 341-352.
33 Van der Hoeven T.A., Coon M.J. *J. Biol. Chem.* **1974,** 249, 6302-6310,
34 Lowry O.H., Rosebrough N.J., Farr A.L., Randall R.J.: Protein measurement with Folin phenol reagent. *J. Biol. Chem.* **1951,** 193, 265-275,
35 Obach R.S. *Drug Metab. Dispos*. **1999,** 27, 1350-1359,
36 Houston J.B. *Biochem. Pharmacol.* **1994,** 47, 1469-1479,
37 Chiba M., Ishii Y., Sugiyama Y. *AAPS J.* **2009,** 11, 262-276,
38 Davies B., Morris T.: Physiological parameters in laboratory animals and humans. *Pharm. Res.* **1993,** 10, 1093-1095,
39 Chiba M., Shibata Y., Takahashi H., Ishii Y., Sugiyama Y.: Prediction of hepatic clearance in humans from experimental animals and *in vitro* data. in: J.S. Lee, R.S. Obach, M.B. Fisher (Eds.), Drug Metabolizing Enyzmes. Cytochrome P450 and Other Enzymes in Drug Discovery and Development, Fontis Media, Lausanne, Switzerland, **2003**, pp. 453-481

40 Naritomi Y., Terashita S., Kagayama A., Sugiyama Y. *Drug Metab. Dispos.* **2003,** 31, 580-588,
41 Avdeef A.: Absorption and Drug Development Solubility, Permeability and Charge State. pION, Inc. John Wiley & Sons., 2003 ,pp. 116-246.
42 Manfred K., Frank S. and Klaus G. *J. Med. Chem.* ***1998,*** *41 (7), 1007-1010.*
43 Tam K.Y., Takács-Novák K., *Anal. Chim. Acta.* **2001,** 434, 157-167
44 Völgyi G, Ruiz R, Box K, Comer J, Bosch E, Takács-Novák K.. *Anal Chim Acta.* **2007**, 583, 418-428
45 Jako, T., Szabo, E., Tabi, T., Zachar, G., Csillag, A., & Szoko, E. *Electrophoresis,* **2014**, 35(19), 2870-2876.